



A TUNED CLC NETWORK ANALYSIS FOR A CLOSED LOOP HYBRID PHASE SHIFT CONTROLLED DUAL ACTIVE BRIDGE CONVERTER

¹Dr. P Arul Kumar, ²Md. Samdani, ³Ms. R. Swathi

¹Associate professors, Department of EEE, Balaji Institute of Technology and science.

²Assistant professors. Department of EEE, Balaji Institute of Technology and science.

ABSTRACT

This paper proposes a resonant dual-active bridge (DAB) converter, which uses a tuned capacitor-inductor-capacitor network. In comparison to the conventional DABs, the proposed topology significantly reduces the bridge currents, lowering both conduction and switching losses and improving the bridge power factors. A mathematical model, which predicts the behavior of the proposed system, is presented to show that both the magnitude and direction of the power flow can be controlled through either relative phase angle or pulse width modulation of voltages produced by the bridges. A mathematical model, which predicts the behavior of the proposed system, is presented to show that both the magnitude and direction of the power flow can be controlled through either relative phase angle or pulse width modulation of voltages produced by the bridges. The viability of the proposed concept is verified through simulation. Experimental results of a 4- kW prototype converter, which has an efficiency of 95% at rated power, are also presented with discussions to demonstrate the improved performance of this topology. In addition, the proposed control plot does not fundamentally build the conduction losses in correlation with the expanded EPS control. In this way, the modified DAB can work efficiently. The topology deduction are first known. At that point, the EPS and TPS regulations are connected, and the comparing working standards and qualities, including the switching, power transfer, and root-mean-square current, are investigated in detail with the help of MATLAB Simulink software with complete results with dynamic response.

1. INTRODUCTION

GLOBALLY there has been an increased concern in the unsustainable manner in which we meet our electrical energy needs. Concerns lie mainly in the way that we are depleting natural resources such as oil and gas while polluting the environment as we extract energy from these unrenewable sources. This has resulted in electricity increasingly being generated from renewable energy (RE) sources like wind, hydro, tidal, and solar [1]–[4], to address these concerns. Conventionally, large-scale RE generation plants, such as solar and wind farms, have been built and incorporated into the main grid. Efforts to reduce transmission losses have resulted in a shift toward microscale distributed generation (DG) from RE sources [5]–[7]. Power generation through microscale distributed RE sources is highly variable in nature mainly due to the dependence of generation on climate conditions

[8]. Some form of energy storage is, therefore, an essential and integral part of most, if not all, RE systems to alleviate the mismatch between electricity supply and demand. Electric vehicles (EVs), which initially emerged as an environmentally friendly and efficient means of transport, can also help to provide power network stability in the presence of these fluctuations when used as vehicle-to-grid (V2G) power sources. EV use in RE systems to supplement energy storage, which is referred to as ‘Living & Mobility’ [9], essentially requires a bidirectional power interface between the local grid and the EVbattery to allow for charging the battery when surplus energy is being generated and for extracting energy when there is a deficit. To facilitate a V2G connection with the utility grid requires the use of an ac-dc converter stage, known as a “grid inverter,” along with a dc-dc converter, which is also required to be



bidirectional. The grid inverter is controlled to maintain a constant dc-link voltage either by extracting power from the grid or delivering power to the grid. When the dc–dc converter is delivering power to the load, the grid inverter functions as a rectifier, whereas when the power flow is reversed it works as an inverter generating power at grid frequency.

GLOBALLY there has been an increased concern in the unsustainable manner in which we meet our electrical energy needs. Concerns lie mainly in the way that we are depleting natural resources such as oil and gas while polluting the environment as we extract energy from these unrennewable sources. This has resulted in electricity increasingly being generated from renewable energy (RE) sources like wind, hydro, tidal, and solar [1]–[4], to address these concerns. Conventionally, large-scale RE generation plants, such as solar and wind farms, have been built and incorporated into the main grid. Efforts to reduce transmission losses have resulted in a shift toward microscale distributed generation (DG) from RE sources [5]–[7]. Power generation through micro scale distributed

RE sources is highly variable in nature mainly due to the dependence of generation on climate conditions [8]. Some form of energy storage is, therefore, an essential and integral part of most, if not all, RE systems to alleviate the mismatch between electricity supply and demand. Electric vehicles (EVs), which initially emerged as an environmentally friendly and efficient means of transport, can also help to provide power network stability in the presence of these fluctuations when used as vehicle-to-grid (V2G) power sources. EV use in RE systems to supplement energy storage, which is referred to as ‘Living & Mobility’ [9], Essentially requires a bidirectional power interface between the local grid and the EV battery to allow for charging the battery when surplus energy is being generated and for extracting energy when there is a deficit. To facilitate a V2G connection with the utility grid requires the use of an ac–dc converter stage, known as a “grid inverter,” along with a

dc–dc converter, which is also required to be bidirectional. The grid inverter is controlled to maintain a constant dc-link voltage either by extracting power from the grid or delivering power to the grid. When the dc–dc converter is delivering power to the load, the grid inverter functions as a rectifier, whereas when the power flow is reversed it works as an inverter generating power at grid frequency. Of the many converters developed, both wired and wireless options, dual-active bridges (DABs) are gaining popularity as a preferred option for interfacing EVs with the grid. DABs facilitate bidirectional power transfer with galvanic isolation, have a high power density and can accommodate a wide range of voltages by operating in both buck and boost modes. Early DAB converters were controlled using singlephase- shift (SPS) control to allow for bidirectional power transfer at variable power levels. SPS control, however, leads to a high reactive current in the system, especially when there is an imbalance in voltages. This high reactive current leads to increased conduction losses in the devices decreasing the overall system’s efficiency. Various modulation schemes were investigated in an effort to reduce the switch current stresses and the attendant switching and conduction losses. These required a more complicated control system than that used with the conventional SPS control.

Various DAB converters employing a form of series resonance have been investigated, some with phase control and fixed frequency and some with frequency control. In a correlation with frequency of DAB variation in [4], the authors reasoned that the main preferred of the last was its lower current effect and reduced losses. Also, series resonant DABs typically require a more complex control system, particularly when they are required to operate with wide load and supply voltage variations. All current AB converters in a general draw a high current at full power component, and along these lines, bring losses. As an answer, this paper displays a novel

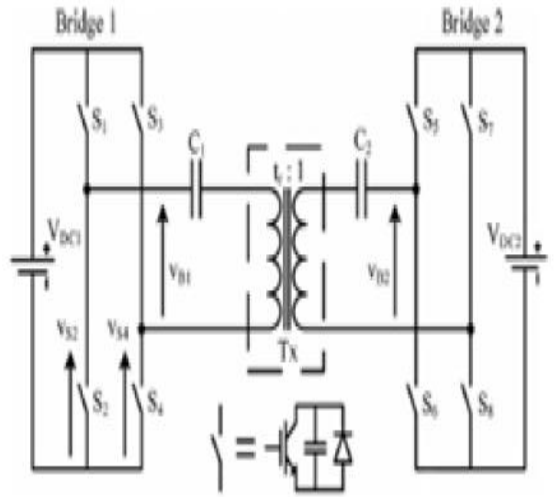


Fig. 1. Proposed Resonant DAB Converter DAB converter topology, which uses a system to limit the power in bridges. While the proposed converter is conceptually similar to the LCL DAB proposed in [7], including the simple control scheme employed, this variant employs a tuned capacitor-inductor-capacitor (CLC) network. Also, response of CLC system to voltages delivered by the full-bridge converters is fundamentally unique to that of a DAB utilizing a LCL system. The tuned CLC influences a reduce in magnitude of currents and losses. PWM of single bridge is utilized to control power flow, while phase shift between bridges settled at 90° or -90° , as indicated by direction of power required. The simulated results together with experiment results acquired from a 4-kW model system, to show the capacity of the proposed topology to exchange bidirectional power at a high productivity for an extensive variety of dc supply voltages and power.

2. PROPOSED RESONANT DAB

The structure of the proposed resonant DAB (RDAB) converter is shown in Fig. 1. There are two full-bridge converters, each of which operates at a fixed switching-frequency f_s , and outputs a three-level pulse widthmodulated voltage source from its dc supply. The bridges are coupled with a resonant network comprising C_1 , C_2 , and transformer T_x , which also

provides galvanic isolation. T_x has leakage and mutual inductances L_1 and L_2 (see Fig. 3), which are an integral part of the resonant network, which is tuned to the fundamental of the switching frequency, as given by

$$(L_1 + L_2)C_1 = L_2C_2/t_r^2 = \frac{1}{\omega_s^2} = \frac{1}{(2\pi f_s)^2}$$

An alternative implementation would use a tightly coupled transformer, having minimal leakage inductance, with a discrete inductor in series with the primary. Fig. 2 illustrates the switching sequences used to control the RDAB converter's power flow. All bridge switches are operated with 50% duty at the switching frequency f_s , with antiphase switching of the transistors within a leg. A phase displacement

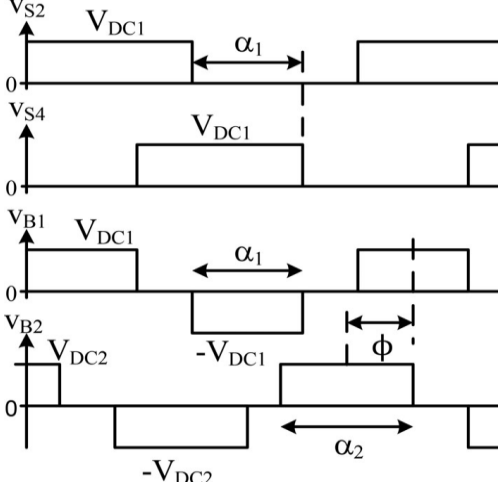


Fig. 2. Bridge voltage waveforms

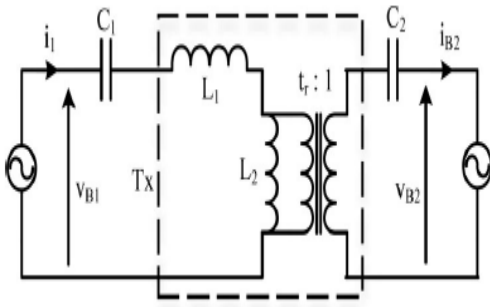


Fig. 3. Initial model. α_1 between the legs of Bridge 1 is used to affect PWM of its output voltage V_{B1} , the



difference between its leg voltages, as shown in the first three plots. As α_1 changes from 0° to 180° VB_1 's duty changes from 0 to 50%, the latter's square waveform corresponding to 100% modulation. VB_2 is obtained from Bridge 2 in a similar manner, using modulation α_2 . The phase-shift ϕ between VB_1 and VB_2 determines the direction of the power flow, and is set to either 90° or -90° , for forward and reverse operation, respectively.

3. CONTROL AND MODES OF OPERATION

In the first step, the EPS modulation [7] is applied to the modified DAB converter. The gate drive sequences of switches and definition of two phase-shift angles are illustrated in Fig. 4, where $u_s = u_2 + u_3 = 2u_T$, and u_T represents the ac voltage applied to the transformer magnetizing inductance. Neglecting the dead time, the upper and lower switches in each switching leg are driven complementarily with a duty cycle of 0.5. The two primary-side switching legs are out of phase, the two secondary-side switching legs are driven synchronously, and the phase-shift angle between the primary and secondary units is θ . With the EPS control, u_1 is characterized as an ac rectangular wave with amplitude V_p , and both u_2 and u_3 are ac square waves with the same amplitude V_s ($V_s = nV_s$). Depending on the relationship between the rising edges of u_1 and u_s , three different operating modes can be identified, as shown in Table I. Operating mode I occurs in both forward and reverse operation. Ignoring the dead time, one switching cycle can be divided into six stages, as shown in Fig. 4. Mode I is taken as an example to explore the operation of the modified DAB converter with the EPS control, and due to symmetry, only three stages over the half switching cycle $[0, \delta]$ are detailed below.

As aforementioned, the three inductor currents i_1 , i_2 , and i_3 can be derived with the superposition of the three decoupled currents i_{12} , i_{23} , and i_{31} which derived by voltages across equivalent inductors L_{12} , L_{23} , and L_{31} as in Fig. 4. Since the two equivalent ac voltage sources u_2 and u_3 are synchronous

always in the EPS control, the voltage across L_{23} is zero, and the ac current i_{23} is equal to 0 in stages. Therefore, i_{12} equals 0 as well, which means that no current flows through the inserted secondary-side inductor in EPS control, and the operation is the same as the conventional DAB converter. Stage 1 $[0, \alpha]$ [see Fig. 4 prior to this stage, S_{p2} , S_{p3} , S_{s2} , and S_{s3} have been conducting. At the onset of this interval, S_{p2} is turned OFF and

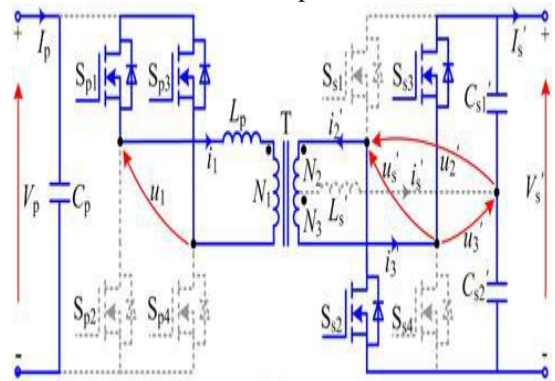


Fig. 4. Stage 1 Operation

theoretically S_{p1} is turned ON with ZVS if $i_1(0) < 0$ which means that the antiparallel diode of S_{p1} conducts before the transistor does. This interval ends up with S_{s2} and S_{s3} being turned OFF. During this interval, the two currents i_{12} and i_{31} are expressed as

$$i_{12}(\theta) = i_{12}(0) + \theta$$

$$i_{31}(\theta) = i_{31}(0) - \theta.$$

Stage 2 $[\beta, \alpha]$ [see Fig. 3 at β , S_{s2} and S_{s3} are turned OFF, and theoretically S_{s1} and S_{s4} are turned ON with ZVS if $i_2(\beta)$ and $i_3(\gamma)$ are negative. This interval ends up with S_{p3} being switched OFF at α . During this stage, i_{12} and i_{31} are $i_{12}(\theta) = i_{12}(\beta) - (\theta - \beta)$ $i_{31}(\theta) = i_{31}(\beta) + (\theta - \beta)$

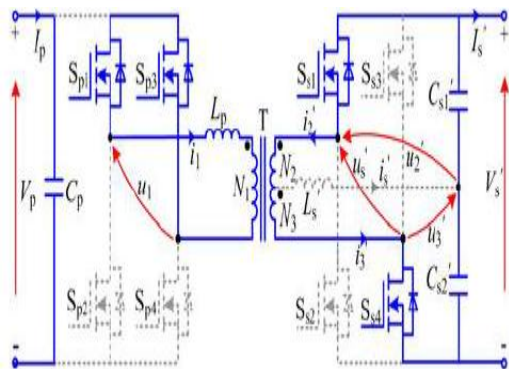


Fig. 5. Stage 2 Operation Stage 3 [α, π] [see Fig. 6 at α , Sp3 is turned OFF, and Ss1 is triggered ON with ZVS if $i_{12}(\alpha)$ is negative. This interval ends up with Sp1 being switched OFF at π . During this stage, i_{12} and i_{31} are $i_{12}(\theta) = i_{12}(\alpha) + (2k - 1)(\theta - \alpha)$ $i_{31}(\theta) = i_{31}(\alpha) - (2k - 1)(\theta - \alpha)$ Where the voltage conversion ratio $k = V_p / (n \cdot V_s)$. Thus, i_1, i_2 , and i_3 are derived as $i_1(\theta) = i_1(\alpha) + 2(2k - 1)(\theta - \alpha)$ $i_3(\theta) = i_2(\theta) = i_2(\alpha) - (2k - 1)(\theta - \alpha)$.

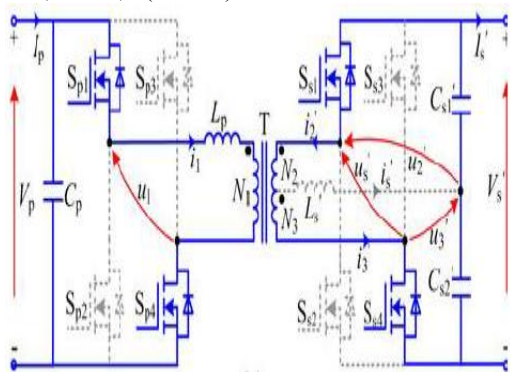


Fig. 6. Stage 3 Operation Due to modulation symmetry, the upper and lower switches of each switching leg have the same soft-switching condition. Therefore, only Sp1, Sp4, Ss1, and Ss4 are considered, and their switching instants and ZVS conditions are listed in Table II. In order to achieve ZVS operation, the corresponding inductor current at each switching instant should be no more than $-IZVS$, where $IZVS$ is the minimum current for achieving ZVS within a specified short dead time interval. With the EPS control, time instants β and γ overlapped completely, as shown in Fig.6. By virtue of (10), (12), and

(14), the normalized switching currents for each operating mode can be found, as shown in Table III. Theoretically, ZVS turn-on of all devices can be achieved if the inductor currents at four switching instants are less than 0, i.e., $IZVS=0$ in Table II. Applying ZVS conditions in Table 2, constraints in Table 1 to equations in Table 3, we find phase-shift angle ϕ_p should satisfy

$$\phi_p = \pi (1 - 1 / (2k)).$$

CONCLUSION

A novel DAB topology that employs a *CLC* resonant network has been described. The mathematical model presented has been shown to accurately predict the performance of the proposed topology. Although, the RDAB presented in this paper has not been optimized for efficiency, the results of a 4-kW prototype operated under various conditions suggest a significant improvement in performance in comparison to a conventional DAB converter with SPS control. The lower bridge currents of the resonant DAB topology result in an increased power capacity and a higher efficiency over a wide range of bridge dc supply voltages. In comparison with the conventional converter's hardware, the RDAB converter requires the addition of two relatively low-cost capacitors and for these to be tuned with the transformer. As a bonus, these capacitors provide dc current reset, preventing core saturation in the event of abnormal operating conditions. In regard to tuning, it has been shown that the converter's operating characteristics are not particularly sensitive to variations in the component values. There is the potential to further increase the operating efficiency by employing a purpose-designed transformer employing a magnetic shunt to affect the required leakage inductance. This transformer will be smaller than that of a conventional DAB converter on account of the lower operating currents.

REFERENCES

[1] M. H. Nehir, C. Wang, and S. R. Guda, "Alternative energy distributed generation: Need for multi-source operation," in Proc. North Amer. Power Symp., 2006, pp. 547-551.



- [2] T. J. Hammons, J. C. Boyer, S. R. Conners, M. Davies, M. Ellis, M. Fraser, E. Holt, and J. Markard, "Renewable energy alternatives for developed countries," *IEEE Trans. Energy Convers.*, vol. 15, no. 4, pp. 481–493, Dec. 2000.
- [3] P. K. Katti and M. K. Khedkar, "Fostering the use of low impact renewable energy technologies with integrated operation is the key for sustainable energy system," in *Proc. Joint Int. Conf. Power Syst. Technol. IEEE Power India*, 2008, pp. 1–8.
- [4] J. L. Sawin. (2014, Aug. 13). *Renewables 2013 - Global Status Report*. [Online]. Available: http://www.ren21.net/portals/0/documents/resources/gsr/2013/gsr2013_lowres.pdf
- [5] U. K. Madawala, D. J. Thrimawithana, X. Dai, and D. M. Vilathgamuwa, "A model for a multi-sourced green energy system," in *Proc. IEEE Conf. Sustainable Energy Technol.*, 2010, pp. 1–6.
- [6] J. Marsden, "Distributed generation systems: A new paradigm for sustainable energy," in *Proc. IEEE Green Technol.*, 2011, pp. 1–4.
- [7] R. Ramakumar and P. Chiradeja, "Distributed generation and renewable energy systems," in *Proc. 37th Intersoc. Energy Convers. Eng. Conf.*, 2002, pp. 716–724.
- [8] S. I. Mustapa, Y. P. Leong, and A. H. Hashim, "Issues and challenges of renewable energy development: A Malaysian experience," in *Proc. Int. Conf. Energy Sustainable Develop. Issues Strategies*, 2010, pp. 1–6.
- [9] W. Kempton and S. Letendre, "Electric vehicles as a new power source for electric utilities," *Transp. Res. Part D, Transport Environ.*, vol. 2, pp. 157–175, 1997.
- [10] B. Kramer, S. Chakraborty, and B. Kroposki, "A review of plug-in vehicles and vehicle-to-grid capability," in *Proc. IEEE Ind. Electron.*, 2008, pp. 2278–2283.